Influence of Hair Density and Hair Length on Interparticle Interactions of Spherical Polymer Brushes in a Homopolymer Matrix

Lee Yezek, Wolfgang Schärtl,* Yongming Chen, Kerstin Gohr, and Manfred Schmidt

Institut für Physikalische Chemie, Universität Mainz, Welderweg 11, 55099 Mainz, Germany

Received July 23, 2002; Revised Manuscript Received April 8, 2003

ABSTRACT: The dynamics of hairy spherical nanoparticles in a melt of linear polymer chains has been investigated by mechanical spectroscopy as a function of particle topology and concentration. Using a simple free volume approach for the data analysis of the structural relaxation time vs concentration and the well-known hard-sphere result as a reference, a semiquantitative measure for the interparticle interactions, that is particle deformability/softness, and the effective particle size compared to the size of a nonswollen spherical brush has been determined. For these studies, model particles of hairy nanoparticles differing in either hair length or grafting density have been prepared. In contrast to our previous studies of copolymer micelles, for the new graft particles at very high grafting densities our free volume approach led to nonphysical results: the effective particle size is increasing with increasing concentration. Therefore, it has been concluded that densely grafted hairy particles in a matrix of linear polymer chains cannot be mapped onto a hard-sphere reference system, indicating that the interaction potential is not simply soft repulsive.

Introduction

Spherical nanoparticles with polymer brush surfaces in a melt of homopolymer chains not only are an important system for technical applications, e.g., as mechanically enhanced thermoplastic polymers or scratch-resistant coatings, but also provide a very important new model system in the field of soft colloidal particles. Previous investigations of frozen copolymer micelles with polystyrene (PS) core and polyisoprene (PI) corona in a matrix of linear polyisoprene chains[1,2] have enabled us to quantify the effective particle size and the apparent particle softness by a free volume approach, that is, fitting the dependence of structural relaxation, inverse viscosity, or diffusion coefficient of the micelles with the Doolittle equation:[3]

$$\frac{X}{X_0} = \exp\left(-\frac{\kappa}{\phi^{-1} - \phi_0^{-1}}\right) \tag{1}$$

Here, X is a physical quantity related to the particle mobility (either diffusion coefficient, inverse zero-shear viscosity, or inverse structural relaxation time) at given particle concentration ϕ, κ is a parameter characterizing the divergence in particle dynamics while approaching the liquid−solid transition and therefore a direct measure for the particle softness or compressibility (hard spheres: $\kappa = 1.6$[4]), and ϕ_0 is the particle volume fraction at the liquid−solid transition, that is, where the structural relaxation dynamics of the system is frozen ($X = 0$). Originally applied to dispersions of hard spherical colloids,[5] eq 1 should be valid to describe any isotropic system that exhibits a repulsive interparticle interaction potential and, as a direct consequence, with increasing particle concentration approaches a liquid−solid transition due to a lack in free volume. Our previous studies of copolymer micelles in a homopolymer melt which showed soft-repulsive interactions[1,2] have nicely demonstrated the applicability of this new approach. It has been shown that the molecular weight of the matrix chains with respect to the hair length has a strong influence on the parameters of eq 1: whereas the particle softness (and κ) increases with decreasing molecular weight of the matrix, ϕ_0 decreases, which corresponds to an increase in effective particle size. We have explained these results by the more effective swelling of the corona for short matrix chains (wet brush) in comparison to long matrix chains (dry brush), as already theoretically predicted.[6] These earlier wet-brush systems showed a systematic decrease in effective particle size with increasing concentration, which has been interpreted as deswelling and/or particle deformation.[2]

It is interesting to compare our approach using the Doolittle equation (eq 1) to describe the dependence of structural relaxation on particle concentration with an analysis of rheological data of spherical colloids interacting via a soft-repulsive potential published previously by Buscall et al.[7,8] These authors used the Krieger−Dougherty equation[9,10] to describe the dependence of the normalized zero-shear viscosity on particle concentration.

$$\eta_R = \left(1 - \frac{\phi}{\phi_0}\right)^{-[\eta]\phi_0} \tag{2}$$

Here, η_R is the normalized viscosity of the dispersion and $[\eta]$ is the intrinsic viscosity which provides a quantitative measure for the deformability of the brush layer and therefore for the softness of the interparticle interactions. As in eq 1, ϕ_0 is the particle volume fraction where the viscosity appears to diverge, i.e., at the liquid−solid transition. Very interestingly, the authors spent some effort how to define the volume fraction ϕ. One might simply take ϕ as the volume fraction of the colloidal hard cores. In this case, the effect of the softness of the brush layer is subsumed in the fitting

* To whom correspondence should be addressed. E-mail schaertl@mail.uni-mainz.de.

10.1021/ma021179w CCC: $25.00
Published on Web 05/09/2003

parameters $[\eta]$ and ϕ_0, which therefore become system dependent. This is similar to our approach: in eq 1, we have defined ϕ as the volume fraction of the nonswollen dry brush and estimate the degree of swelling by direct comparison with a hard-sphere reference system (vide infra). A more sophisticated approach is to measure the intrinsic viscosity of the system and to define ϕ as an effective volume fraction according to

$$\phi = \phi_{\text{eff}} = 2c[\eta]/5 \tag{3}$$

with c the concentration of the particles in g/mL. This approach may be valid for dilute particle dispersions or, more general, dispersions where the brush thickness is not changing much with particle concentration. However, it clearly does not take into account the strong compression of the brush layer with increasing particle concentration found for very soft particles, which leads to a decrease of the effective particle size as we have detected previously for our micellar system: eq 3 predicts $\phi \sim c$, which is not fulfilled if the particles are effectively shrinking with increasing c. Let us try to compare the two different approaches in detail:

$$\eta_R = \left(1 - \frac{\phi_{\text{eff}}}{\phi_{\text{eff},0}}\right)^{-[\eta]\phi_{\text{eff},0}} = \exp\left(\frac{\kappa}{\phi_{\text{dry}}{}^{-1} - \phi_{\text{dry},0}{}^{-1}}\right) \tag{4}$$

Here, ϕ_{eff} is the effective particle volume fraction defined in eq 3, and $\phi_{\text{eff},0}$ is the effective volume fraction at the liquid−solid transition. On the other hand, ϕ_{dry} is the volume fraction of the nonswollen dry brush corresponding directly to the solid particle concentration c, and $\phi_{\text{dry},0}$ is the solid particle volume fraction at the liquid−solid transition. For simplification, let us assume identical particle and matrix densities; therefore $\phi_{\text{dry}} = c$. In the dilute regime $\phi_{\text{eff}} \ll \phi_{\text{eff},0}$, $c \ll \phi_{\text{dry},0}$ eq 4 leads to

$$[\eta]\phi_{\text{eff}} = [\eta]^2(2/5)c = \frac{\kappa}{c^{-1} - \phi_{\text{dry},0}{}^{-1}} \tag{5a}$$

or

$$[\eta]^2 \sim \frac{\kappa}{1 - c/\phi_{\text{dry},0}} \tag{5b}$$

Taking into account $c \ll \phi_{\text{dry},0}$, we finally get $[\eta]^2 \sim \kappa$. Therefore, κ indeed seems to be a measure for the extension and deformability of the polymer brush layer and the corresponding particle softness, as claimed above.

Buscall et al. have found that smaller colloidal particles showed a liquid−solid transition at an effective volume fraction of about 0.64 in the limit of low frequencies (zero-shear viscosities).[7] The same effective volume fraction is assumed in our free-volume approach in respect to a hard-sphere reference, which therefore seems to be justified. In addition, one can estimate the effective volume swelling of the particles by comparing the core volume fraction and the effective volume fraction given in Figure 1 of ref 7. This swelling increases with decreasing particle size or increasing curvature, corresponding to the increase in brush thickness with decreasing core radius theoretically predicted by Lin and Gast.[11] Note, however, that the studies of Buscall et al., like all other papers published in the field of dispersions of sterically stabilized colloidal particles, in comparison to our system comprise much larger particles with much shorter hairs, dispersed in a molecular solvent. Consequently, the interparticle interactions in this case are expected to be purely repulsive. An exception are studies of ternary systems, i.e., large colloidal particles in a molecular solvent with added polymer chains, where attractive interparticle interactions based on depletion[12,13] are found. However, we are studying a binary system of colloidal particles in a polymer melt, where this depletion attraction following the argument of Joanny et al.,[14] i.e., the range of the depletion attraction is given by the blob size of the polymer in solution, should vanish. In our case, particle core, hair layer, and solvent are all of comparable size. In contrast to simple colloidal dispersions, the interaction potential in this case may become more complicated and even include an attractive minimum, which is not based on depletion as for the ternary systems mentioned above.

Although polymer brushes have been investigated for more than 20 years by several authors, comparing our experimental results with theoretical predictions is a difficult task. There exist very detailed descriptions of flat brushes, based on the scaling approach of Alexander[15] and de Gennes[16] or on self-consistent-field (SCF) analysis.[17−19] These 2d systems show a parabolic density profile of the tethered layer. Star polymers, that is, polymer brushes with very high curvature and polymer brush thickness much larger than the core dimensions, have been described theoretically by Daoud and Cotton.[20] Here, the density profile of the brush follows a power law. Much less work has concentrated on the intermediate case of a spherical brush with core and brush thickness comparable in size. First SCF calculations based on a lattice model to determine the density profile of curved brushes have been performed by Wijmans et al.[17] Extended calculations from the same group using a cylindrical coordinate system lead to the prediction that the interactions between spherical brushes are far less repulsive than would be expected from the interaction between two equivalent flat surfaces.[21] Very detailed SCF calculations of density profiles and interparticle interactions between spherical brushes immersed in a molecular solvent have been published by Lin and Gast.[11] The authors varied the radius of curvature of the core of the spherical brush, the length of the brush hairs, and their grafting density over a wide range. The interactions between spherical brushes have been found to be purely repulsive, range and softness depending on the size of the core (i.e., the curvature of the brush), the length of the tethered chains, and their grafting density. More recently, however, Roan and Kawakatsu[22] developed a new SCF calculation method which takes into account a redistribution of segment density along the direction parallel to the particle surface in case two interacting spherical brushes approach each other. These authors claim that, since all other theories so far neglected this effect, none of the previous approaches can be applied to the description of spherical brushes with core size 10−100 nm and brush hair length of about the same size, that is, exactly in the regime where our particles are. The new approach leads to rather unusual phenomena not found in other papers about polymer brushes in a molecular solvent; even attractive interaction potentials between spherical brushes have been predicted.

An additional complication of our system is that the spherical brushes are not embedded in a simple molecular solvent, but in a melt of homopolymer chains. Consequently, wetting of the brush by the homopolymer has a major influence on the interparticle interactions. Whereas such wetting phenomena have been discussed for planar brushes,[16,23−27] large spherical cores[28] or, on the other extreme, star polymers,[6] in some detail, we have not been able to find any detailed theoretical predictions for our system where the core of the brush, the brush layer thickness, and the solvent are of the same size. Ferreira et al. found a general scaling criterion that entropic attraction between two flat polymer brushes exists if $\sigma\sqrt{N} > (N/P)^2$, with σ the hair density, N the polymerization degree of the hairs, and P the polymerization degree of the matrix polymer.[27] In simple words, flat polymer brushes with very high grafting density embedded in a matrix of long polymer chains should exhibit attractive interactions. Ferreira et al. found also that flat brushes should attract each other in the case of very low grafting densities provided they are embedded in a matrix of comparatively long polymer chains. For spherical particles by 1 order of magnitude larger than in our case, dispersed in a melt of long polymer chains, Hasegawa et al.[28] have found by mean-field calculations that the interaction potential of the brushes showed an attractive minimum which becomes very shallow at an intermediate grafting density. At lower or higher grafting densities, the attractive interactions become stronger, and the particles form clusters within the polymer matrix. Although there exist a variety of theoretical predictions concerning the interactions between polymer brushes in a polymer melt, it will be very difficult to give a more than qualitative comparison with existing theoretical predictions for our nanoscopic spherical system. However, we should stress here once more that such nanoscopic polymer brushes in a polymer melt play a very important role in industrial applications, and therefore an extension of existing theoretical models to such systems is highly desirable.

Whereas our previous investigations all dealt with particles with identical hair density and comparatively long hairs (about 250 hairs of molecular weight $M >$ 50 000 g/mol on a solid PS core of 10.5 nm radius),[1,2] here we address the influence of the hair density on particle swelling and softness. For this purpose, a direct comparison of particles with identical hair length but a large difference in hair density will be presented.

Experimental Section

Materials. Spherical polyorganosiloxane nanoparticles of radius about 10 nm have been prepared by polycondensation of trimethoxymethylsilane in aqueous emulsion.[29] The particle surface has been end-capped with a bromobutyrate−silane which serves as a polymerization initiator for grafting-from of styrene from the particle surface by atom transfer radical polymerization (ATRP).[30] By this procedure, grafting density and hair length could be adjusted while obtaining a comparatively low polydispersity of the hairs (ratio of weight- to number-average molecular weight $M_w/M_n < 1.5$). Here, it should be noted that impurities originating from the synthesis, e.g., ATRP reagents or surfactants, might influence the interparticle interactions of our spherical brush system. Therefore, all samples have been purified carefully by column chromatography. The samples have been characterized by static and dynamic light scattering of the cores and the spherical brushes, respectively, yielding the particle size and the total particle mass. To determine the grafting density and the hair length, the hairs that are attached to the particle surface via an ester bond have been cleaved from the particle cores and analyzed separately. Finally, it should be mentioned that elementary analysis yielded a Br content of still 60%; i.e., out of 100 hairs about 60 carry a Br atom at the chain end. This Br content might influence the interparticle interaction potential. However, since our findings are consistent with similar results found for much larger latex particles,[28] at present we believe that the small amount of Br atoms at the particle surface (only a few hundred atoms), located at the chain end of PS chains of molecular weight > 13 000 g/mol, at the surface of spherical particles of radius > 15 nm (polyorganosiloxane core plus PS hair corona) should play no significant role for the interpretation of our experimental data as discussed further below.

Table 1. Sample Characteristics As Determined by Dynamic Light Scattering (Core Radius *R*), Static Light Scattering, and Gel Permeation Chromatography (Hair Molecular Weight (Number-Average M_n), Measured after Cleavage of Hairy Spheres (Systems I−III) and Separation of Hairs and Colloidal Cores by Dialysis)[a]

sample	R [nm]	M_n [g/mol]	N_H	D_g [nm^{-2}]	σ	N	$\sigma\sqrt{N}$
system I	11.8	13 300	509	0.29	0.65	28	3.5
system II	11.8	23 800	426	0.24	0.55	50	3.9
system III	10.7	27 700	150	0.10	0.23	59	1.8
PS−PI-mics	10.5	51 400	250	0.18			

[a] The number of hairs per particle N_H has been determined by static light scattering and refractive index measurements as published elsewhere. D_g is the grafting density calculated from R and N_H. σ is the grafting density per unit area, and N is the number of Kuhn lengths (each of length b) per grafted chain.

Table 1 summarizes the characteristics of the samples (hairy spheres) used in our studies. The average grafting density (D_g = number of hairs per nm^2 of particle core surface) has been calculated from the particle core radius R and the number of hairs per particle N_H. For comparison, the characteristics of our previously studied PS−PI micelles[1,2] are also presented in the table. It should be noted that the grafting densities of the new systems I and II lie well above that of the micellar system, whereas system III has a considerably lower hair density.

Homogeneous blends of hairy particles and polymer chains (polystyrene, M = 600, 2000, and 3800 g/mol) have been prepared by solution-casting from tetrahydrofuran. To completely remove the solvent, as-cast films have been annealed at 120 °C, which is well above the glass transition temperature T_g of the matrix and hair polymers, for several hours.

In all cases, the matrix chains are much shorter than the polymer hairs of the brushes, that is, the ratio of the polymerization degree of the matrix chains to the polymerization degree of the hairs $P/N < 0.25$. According to the diagram of states predicted for planar brushes by scaling laws,[23,24,26] we would expect a swollen wet brush at intermediate grafting densities, a nonswollen dry brush at very high grafting densities, and a nonswollen mushroom phase at very low grafting densities. For comparison with theoretical predictions, the grafting density per unit area (defined by the size of the polymer segments) has to be calculated. The unperturbed chain dimension of polystyrene is l [nm] = $0.069M^{0.5}$, with l the end-to-end distance in nm and M the molecular weight of the polymer chain in g/mol. Regarding our PS chains as flexible polymers consisting of Kuhn segments of length b and therefore assuming $l = bP_N^{0.5}$, we obtain an effective polymerization degree $P_N = (0.069^2/4)M$. The grafting density σ is given by eq 6.

$$\sigma = \frac{N_H b^2}{4\pi R^2} \tag{6}$$

with R the particle core radius and N_H the number of hairs per particle (see above). We could not find a single well-defined

value for the Kuhn segment length b of polystyrene in the literature. Our choice is $b = 1.5$ nm, determined from the values given in the *Polymer Handbook* for unperturbed chain dimensions of PS at Θ-conditions (solvent cyclohexane at temperature $T = 34.5$ °C). To compare our three systems with the scaling predictions, we have calculated $\sigma\sqrt{N}$ using eq 7.

$$\sigma\sqrt{N} = \frac{1.5N_H}{4\pi R^2}\,0.0509M_n \tag{7}$$

with M_n the number-average molar mass of the hairs. Results are also given in Table 1. The reader should note the extremely high grafting density especially for systems I and II. Such highly grafted particles are only accessible by the grafting-from technique. According to the scaling predictions, we expect a swollen wet brush for system III and a dry brush for systems I and II. In the case of the longest matrix chains ($M = 3800$ g/mol), however, P/N is about 0.14, and system III may get very close to the transition between the wet and the dry brush state.

It should be noted, however, that as already stated above the scaling predictions found in the literature are valid only for 2d systems. Nanoscopic particles with nonnegligible surface curvature should exhibit a diagram of states different from that shown in refs 23, 24, and 26. Since for curved surfaces, in contrast to planar brushes, the tethered chains of the brush gain in free volume with increasing distance from the surface and therefore excluded-volume interactions between neighboring tethered chains are less pronounced, one would expect an increased wetting compared to flat brushes. Therefore, the swollen wet brush regime might extend toward $P/N > 1.0$ and also toward much larger values of $\sigma\sqrt{N}$, whereas for planar brushes it is restricted to $P/N \leq 1.0$. Following the same argument, the wetting of curved brushes should also increase with increasing hair length. This should be kept in mind when we compare our new findings with previous results obtained for copolymer micelles with hair length at least twice that of the present systems.

Mechanical Spectroscopy. Rheological experiments have been performed at the MPI für Polymerforschung, Mainz, using a mechanical spectrometer (Rheometrics RMS 800), with plate−plate geometry and variable plate diameters (6 and 13 mm). The samples were subjected to small oscillatory shear strain, and the resulting stress was measured. Master curves for the real (G', storage modulus) and imaginary (G'', loss modulus) parts of the dynamic complex shear modulus $G^*(\omega) = G'(\omega) + G''(\omega)$ (G' being the elastic and G'' the viscous response of the system) as well as for the dynamic viscosity $\eta(\omega)$ have been obtained using the time−temperature superposition principle (i.e., shifting the data recorded at various temperatures only along the frequency axis).[31] Further, the time-dependent mechanical relaxation modulus $G(t)$ can be obtained from the frequency-dependent moduli $G'(\omega)$ and $G''(\omega)$ according to the approximation technique of Ferry and Ninomiya.[32] All measurements have been performed well above the glass transition temperature of the matrix polymers. The experimental setup and typical signals obtained for our blends are shown in Figure 1. From these signals, two characteristic quantities representing the structural relaxation (see below) of our system are determined: (1) the zero-shear viscosity (plateau value, see arrow in Figure 1) and (2) the structural relaxation time which is given by a stretched double-exponential fit to the intermediate and the slowest relaxation process within the time-dependent modulus $G(t)$, i.e.

$$G(t) = A_1 \exp\left(-\left(\frac{t}{\tau_1}\right)^{\beta_1}\right) + A_2 \exp\left(-\left(\frac{t}{\tau_2}\right)^{\beta_2}\right) \tag{8}$$

A is the amplitude of the relaxation process, β a stretching factor, and τ the relaxation time. Indices 1 and 2 correspond to the intermediate and the slowest relaxation process, respectively. If $\beta < 1$, the relaxation process is not defined by a single relaxation time, potential reasons being spatial heterogeneities within the sample and/or polydispersity of the particles. In this case, an average relaxation time is calculated according to

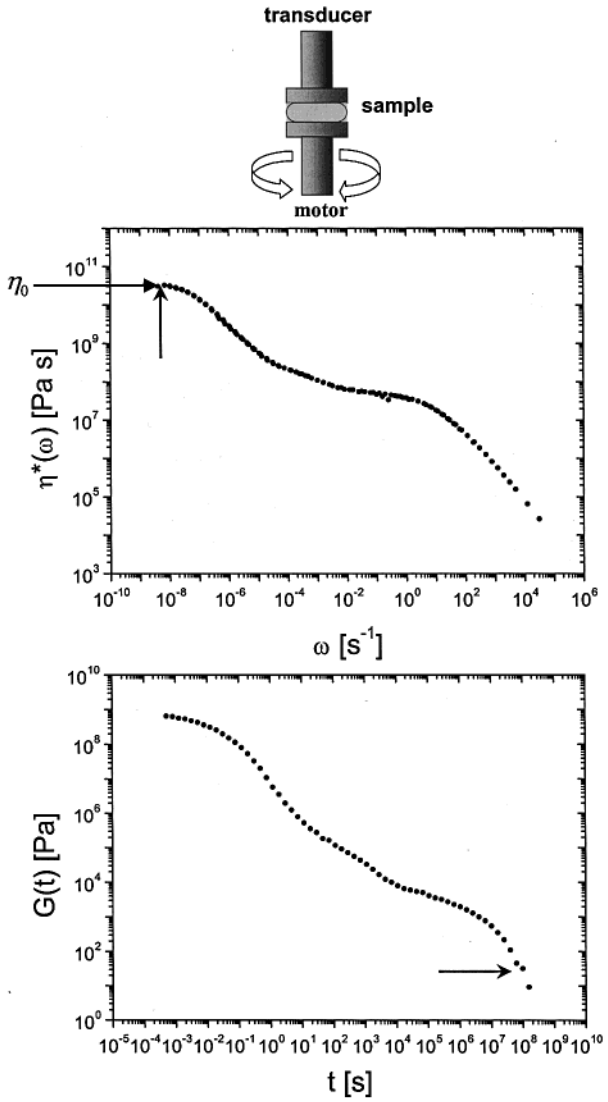

Figure 1. Sketch of the experimental setup of an oscillatory plate−plate mechanical spectrometer and typical experimental results for the frequency-dependent viscosity $\eta^*(\omega)$ and the relaxation modulus $G(t)$ (obtained from system I, concentrated 33 wt % in matrix PS-3800). The arrows indicate the zero-shear viscosity plateau ($\eta^*(\omega)$) and the structural relaxation process ($G(t)$).

$$\langle\tau\rangle = \frac{\tau}{\beta}\Gamma\left(\frac{1}{\beta}\right) \tag{9}$$

with Γ the Gamma function. Some typical fits are shown in Figure 2; the fitting parameters of the slowest process for system I in matrix $M = 3800$ g/mol are given in Table 3. The stretching parameter β is about 0.35 and shows no systematic variation with increasing concentration. This value corresponds to a rather broad distribution of relaxation times; however, we have found similar values in our rheological studies of copolymer micelles. For the micellar system, the self-diffusion coefficients measured by forced Rayleigh scattering were well-defined. Therefore, the reason for the broad distribution of relaxation times found in rheological measurements most probably is not caused by heterogeneities within the sample or particle polydispersity. A possible explanation may be the measurement technique itself: in plate−plate geometry used for our oscillatory shear measurements, the stress acting on the sample is not constant but varies from minimum stress at the sample center to a maximum value at the edges.

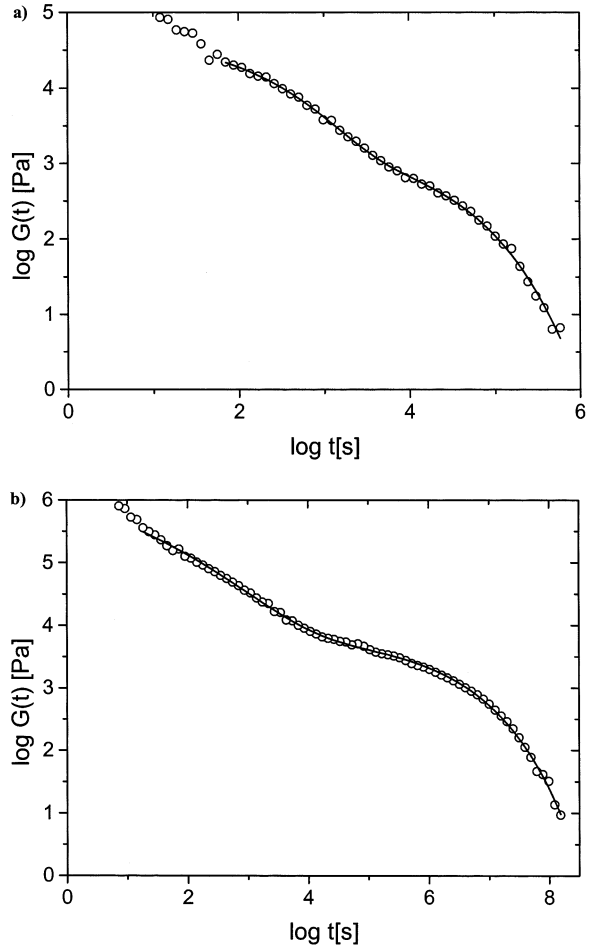

Figure 2. Examples of stretched double-exponential fits (solid lines) to the medium and the slowest relaxation process of $G(t)$ for system I in matrix PS-3800; particle concentration $\phi = 0.20$ (a) and 0.33 (b).

Table 2. WLF Fitting Parameters Used To Determine the Shift Factors for Calculation of $G(t)$ According to the Time−Temperature Superposition Principle (Reference Temperature $T = 92$ °C) for System I in Matrix Polymer $M = 3800$ g/mol in Dependence of Particle Concentration

ϕ	0.10	0.20	0.26	0.30	0.33
C_1	11.3	11.2	11.2	11.4	11.3
C_2	61.1	59.4	61.1	55.4	53.7

Table 3. Fitting Parameters of Stretched Exponential Fits to the Slowest Relaxation Process of $G(t)$ for System I in Matrix Polymer $M = 3800$ g/mol in Dependence of Particle Concentration

ϕ	0.10	0.20	0.26	0.30	0.33
τ [s]	6490	8500	2700	102710	736240
β	0.39	0.42	0.30	0.35	0.35

Especially for the slow structural relaxation process based on center-of-mass motion of the particles (see below), this variation in stress might cause a corresponding variation in relaxation rates and therefore lead to a broad distribution of the measured relaxation times.

Here, some additional comments may be necessary. Figure 1 clearly shows three relaxation processes as found previously for our micellar system. In ref 1, a detailed comparison of the rheological data with dielectric relaxation spectroscopy and self-diffusion measurements by forced Rayleigh scattering unambiguously allowed us to determine the origin of the three processes: the fastest and the intermediate process were due to segmental and structural relaxation of the polymer chains. The slowest process was clearly identified as center-of-mass motion of the particle cores, the relaxation time corresponding to diffusion over a distance comparable to the core size. Similar results based on the comparison of diffusion and rheology of copolymer micelles have independently been found by another group.[33] Since $G(t)$ for our new system of grafted particles dispersed in a polymer melt looks qualitatively identical to our previous results obtained from copolymer micelles, we believe it justified to attribute the slowest relaxation process to a center-of-mass motion of the particle cores, which therefore corresponds to a structural relaxation mode.

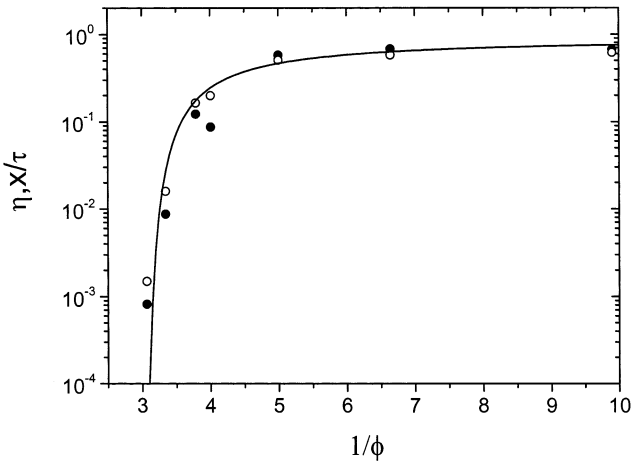

Figure 3. Normalized inverse structural relaxation time (x/τ) (solid circles) and zero-shear viscosity (open circles) plotted vs inverse particle volume fraction ($1/\phi$) (system I in matrix PS-3800). The straight line is the best fit to both data sets according to the Doolittle equation (eq 1).

Another important point concerns the validity of the time−temperature superposition principle used to calculate $G(t)$ over more than 12 decades. It seems to be surprising that this principle holds even for highly filled polymer systems as in our case, where the relaxation characteristics and activation energies could depend strongly on particle concentration. To proof the validity of time−temperature superposition, the WLF parameters for system I in matrix PS-3800 are given in Table 2.

Clearly, there is only a minor nonsystematic variation of C_1 and C_2 with increasing particle concentration. We therefore conclude that the application of the time−temperature superposition principle is justified even in the case of our highly filled polymer systems, and the resulting relaxation curves $G(t)$ are valid for further data analysis.

Results and Discussion

1. Comparison of Zero-Shear Viscosity and Structural Relaxation Time. As stated above, zero-shear viscosity and structural relaxation time both are based on the same physical transport process, namely the diffusion of spherical particles within the polymer matrix. Figure 3 shows the best fit according to eq 1 for the terminal relaxation time and for the zero-shear viscosity plotted vs particle concentration.

Clearly, the two different dynamical quantities can be described by one fitting curve. In the following we will restrict ourselves to the discussion of the terminal relaxation times in dependence of particle concentration. The reader should note, however, that all arguments given below also hold for the zero-shear viscosity.

2. Effect of Matrix Molecular Weight on Structural Relaxation of Densely Grafted Hairy Spheres. In Figure 4, the concentration dependence of the structural relaxation time of a hairy sphere system (system I) with very high grafting density ($D_g = 0.29$ nm^{-2}) (in comparison to the micelles previously studied: $D_g = 0.18$

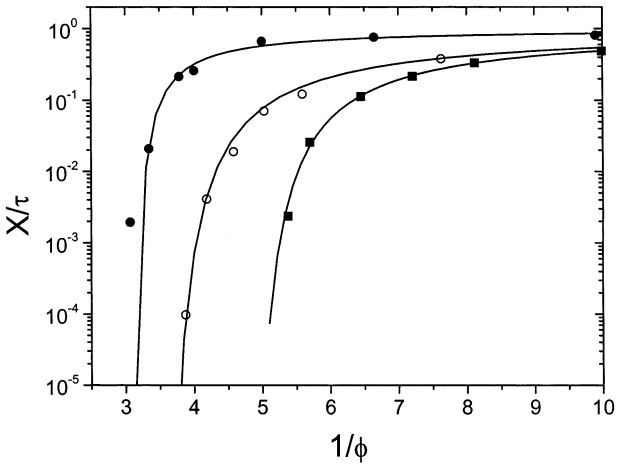

Figure 4. Normalized inverse structural relaxation time (x/τ) vs inverse particle volume fraction ($1/\phi$) (system I in three different matrix polymers: PS-3800 (solid circles), PS-2000 (open circles), and PS-600 (solid squares)). Lines correspond to best fits according to the Doolittle equation (eq 1).

Table 4. Fitting Parameters of Doolittle Fits (Eq 1) for System I in Three Different Matrix Polymers (See Figure 3)

matrix [g/mol]	600	2000	3800
κ	3.8	6.3	1.1
ϕ_0	0.21	0.32	0.33

nm^{-2}), but comparatively short hairs, is shown for blends with three different matrix molecular weights.

As shown in previous studies of copolymer micelles with lower grafting density but much longer hairs, the effective particle volume and also the particle softness strongly increase with decreasing matrix molecular weight (transition dry brush−wet brush). For a quantitative discussion, the fitting parameters of the Doolittle fits (eq 1) are summarized in Table 4. Interestingly, the κ-parameter characterizing the particle softness in the matrix $M_{PS} = 3800$ g/mol is much smaller ($\kappa = 1.1$) than expected although the matrix chains are still more than 3 times shorter than the hairs ($M = 13\,300$ g/mol). Here, it should be noted again that the hard-sphere value for κ equals 1.6. In this respect, densely grafted hairy spheres in a matrix $M_{PS} = 3800$ g/mol show an even steeper decay in structural dynamics while approaching the liquid−solid transition than hard spheres. On the other hand, the hairy spheres clearly show a strong increase in effective volume due to corona swelling, since the particle volume fraction at the solid−liquid transition ϕ_0 equals 0.33 in comparison to a polydisperse ($\Delta R/R = 10\%$) hard-sphere value $\phi_{0,HS} = 0.65$.[34]

In Table 5, we compare the degree of particle swelling ($= \phi_{0,HS}/\phi_0$) at the liquid−solid transition of all three grafted microgel systems with comparatively short hairs and of our previously studied micellar system with different grafting density and much longer hairs. As Table 5 shows, the degree of swelling for the new microgel system I is nearly as expected from the ratio

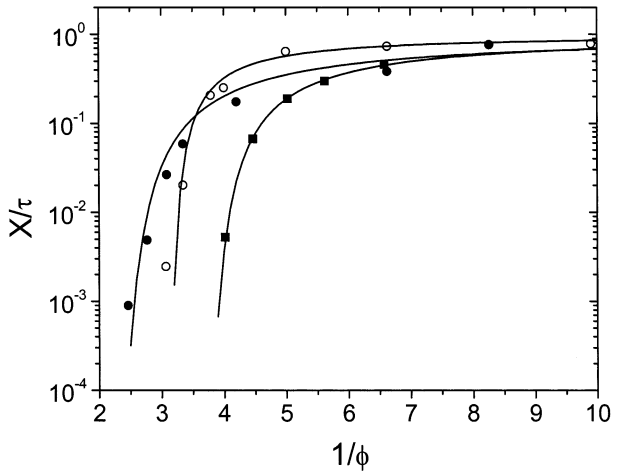

Figure 5. Normalized inverse structural relaxation time (x/τ) vs inverse particle volume fraction ($1/\phi$) [system I (open circles), system II (solid squares), and system III (solid circles), all in matrix PS-3800]. Lines correspond to best fits according to the Doolittle equation (eq 1).

of hair/chain length. System II with comparable grafting density but much longer hairs than system I seems to agree equally well with the swelling behavior of the micellar system as determined from the particle volume fraction at the liquid−solid transition. Interestingly, the swelling behavior of system III with the same hair length as system II but much lower grafting density is much lower than expected from the hair/chain length ratio. However, since the new microgels and the previously studied micelles differ in both hair length and grafting density, for systems I and II the comparable swelling behavior might be pure coincidence, and the effective swelling may in practice depend on both absolute hair length and grafting density. Also, it is difficult to decide whether the relative particle hardness discussed above, in comparison to the previously studied micellar system, is based on the high grafting density or on the low molecular weight of the hairs. To address these important questions, we have investigated the structural dynamics of our three different systems, system II with comparable grafting density as system I (system I: $M = 13\,300$ g/mol, $D_g = 0.29$ nm^{-2}), but twice the hair length (system II: $M = 23\,800$ g/mol, $D_g = 0.24$ nm^{-2}), and system III with nearly identical hair length as system II but much lower grafting density (system III: $M = 27\,700$ g/mol, $D_g = 0.10$ nm^{-2}), in some more detail.

3. Effect of Grafting Density and Hair Length in a Given Matrix. Figure 5 shows the concentration dependence of the structural relaxation time for all three systems investigated in the matrix $M_{PS} = 3800$ g/mol. Clearly, both grafting density and hair length strongly affect particle swelling and particle softness, as can be seen by the distinct differences between all curves.

Qualitatively, it seems that the particle swelling increases both with hair length and with grafting

Table 5. Particle Volume Fraction at the Liquid−Solid Transition (ϕ_0) as a Function of the Ratio Hair to Matrix Chain Length (M_{hairs}/M_{chains}) for Micelles (Long Hairs, Average Hair Density) and Grafted Microgels

M_{hairs}/M_{chains}	46.2	39.7	22.2	10.2	7.3	6.7	6.3	3.5	2.2	1.0
ϕ_0, micelles				0.31					0.40	0.56
ϕ_0, microgels I			0.21			0.32		0.33		
ϕ_0, microgels II		0.13					0.28			
ϕ_0, microgels III	0.25				0.47					

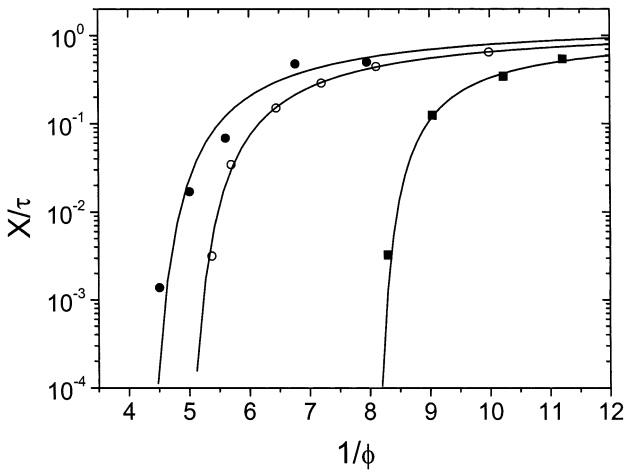

Figure 6. Normalized inverse structural relaxation time (x/τ) vs inverse particle volume fraction ($1/\phi$) [system I (open circles), system II (solid squares), and system III (solid circles), all in matrix PS-600]. Lines correspond to best fits according to the Doolittle equation (eq 1).

Table 6. Fitting Parameters of Doolittle Fits (Eq 1) for Systems I, II, and III in Two Different Matrix Polymers (M = 600 and 3800 g/mol) (See Figures 5 and 6) (e.g., I/600 = System I in Matrix Polymer M = 600 g/mol)

sample	I/600	II/600	III/600	I/3800	II/3800	III/3800
κ	3.8	2.4	3.9	1.1	2.4	3.0
ϕ_0	0.21	0.13	0.25	0.33	0.28	0.47

density. This underlines our previous assumption that densely grafted short haired microgels (system I) and medium grafted long haired micelles only accidentally show a comparable swelling behavior as seen in Table 5. To check whether the effect of the topology of the hairy particles on their swelling behavior is general and the role of the matrix molecular weight is simply to cause a systematic increase in particle swelling and particle softness with decreasing matrix chain length, we have investigated all three systems in two different matrix polymers. Figure 6 shows the structural relaxation behavior in a much shorter matrix (in comparison to Figure 5) M_{PS} = 600 g/mol. For a more quantitative discussion, the fitting parameters for the Doolittle fits shown in Figures 5 and 6 are summarized in Table 6.

First, let us consider the particle softness described by the parameter κ. In the case of the shorter matrix M = 600 g/mol, κ values for systems I and III are nearly identical. Since these particles differ both in grafting density and hair length, this result is surprising. Even more puzzling is the fact that for system II which has much longer hairs but a comparable high grafting density as system I, κ is even smaller. On the other hand, in the case of the longer matrix M = 3800 g/mol, κ is smallest for the particles with the highest grafting density and the shortest hairs (system I), as might be expected. At this stage, it is very difficult to draw final conclusions about the dependence of κ on particle topology. The only thing which can be pointed out is the fact that, in respect to the previous micellar wet brush system with much longer hairs, κ seems to be considerably smaller (wet-brush micelles in matrix M = 22 000 g/mol: κ = 4.8; wet-brush micelles in matrix M = 5000 g/mol (concentration-dependent diffusion coefficients from ref 33): κ = 5.8). Here, we conclude that this behavior is primarily based on the hair length and not on the hair density. The particle softness in this respect is due to the compression and/or interdigitation of dangling hair ends which protrude from a homogeneously swollen corona, a scenario which is consistent with our recent neutron scattering studies of corona profiles of swollen spherical micelles in a homopolymer matrix.

Next, we consider the effective particle size or particle swelling at the liquid−solid transition as described by the parameter ϕ_0. Comparing ϕ_0 of systems I and II, the effective particle swelling clearly increases with increasing hair length. On the other hand, the comparison of systems II and III exhibits a much less trivial result, namely, a strong dependence of particle swelling on grafting density: the system with lower grafting density shows much lower particle swelling. Therefore, we may conclude that both hair density and hair length have a strong influence on the effective particle size or particle swelling by the matrix polymer. Whereas the particle swelling increases with increasing hair length, it also increases with increasing hair density. Our assumptions made in section 2 while discussing the results presented in Table 5 seem to be correct: microgels with short hairs and very high grafting density show comparative swelling behavior as micelles with much longer hairs but lower grafting density due to the compensation of two different topological effects.

4. Model for Hairy Spheres with Different Grafting Densities. The results presented in section 3 are rather surprising. Naively, one would have expected that both particle swelling and particle softness depend on grafting density. Obviously, however, this does not seem to be the case. Here, we will try to give a simple picture why hairy particles with different grafting density (systems II and III) show comparable particle softness (κ) but a large difference in effective particle size or volume swelling (ϕ_0).

Recent neutron scattering studies revealed some astonishing details for the micellar system: particles studied consisted of a glassy polystyrene (PS) core and a polybutadiene (PB) corona of homogeneous density. The effective particle size determined from an analysis of the structure factor part of the scattering curves was found to be much larger (>30 nm) than the extension of the PS core and homogeneous PB corona determined from a form factor analysis in both core and shell contrast (25 nm). In addition, the corona density profile in our case could not be described by the Daoud−Cotton blob model[20] successfully applied to strongly swollen micelles in solution,[35] but the corona showed a constant density. From these experimental results, we concluded that hairy particles in a polymer melt basically consist of three different regions: a solid colloidal core, a corona of homogeneous density, swollen by linear polymer chains, and dangling ends of the corona extending far into the matrix and serving as steric stabilization layer of the particles. Assuming a soft-repulsive potential and analyzing the structural relaxation in reference to a hard-sphere system using the Doolittle equation, the decrease in effective particle size with increasing particle concentration therefore should be caused mainly by changes in the structure of the outer region (compression/interdigitation). As a direct consequence, the particle softness should be determined by the compressibility of these dangling corona chain ends, whereas the particle swelling at the liquid−solid transition should mainly be given by the swelling of the inner corona region with the homogeneous density profile.

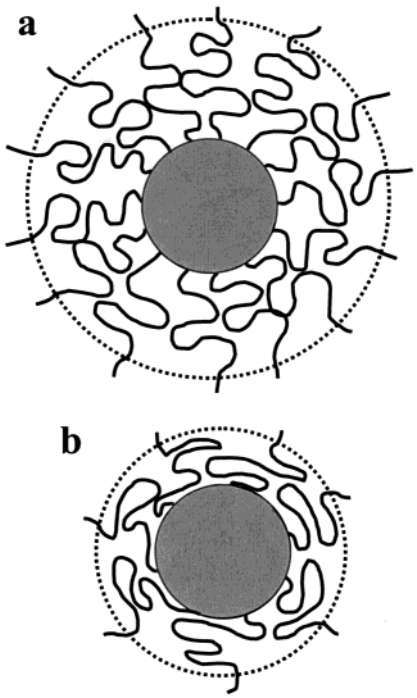

Figure 7. Sketch of spherical wet brushes with high (a) and low (b) grafting density (corresponding to systems II and III, respectively) to illustrate the origin of the comparable particle softness (κ).

Consistent with these recent studies of corona structure and effective particle size of the micellar system, we deduce the following picture for hairy particles with different grafting densities in a polymer melt to explain the experimental results presented in this article.Figure 7 sketches the three regions of our hairy particles with different hair densities (systems II and III): a solid colloidal microgel core, a PS corona layer swollen with homopolymer chains and with a homogeneous density profile, and dangling PS corona ends. In this picture, the dangling ends are viewed as being grafted onto the swollen corona layer with the homogeneous density. First, we admit that this picture still is highly speculative. However, it agrees very well with our recent thorough structural investigations of the strongly related system of copolymer micelles in a homopolymer melt. It also nicely explains all experimental findings presented in this article, as will be seen in the following:

The size of the colloidal cores of systems II and III is 11.8 and 10.7 nm, respectively, leading to grafting densities of 0.24 (system II) and 0.10 (system III) hairs per nm^2. (The reader should keep in mind that the hair density of the micellar system was 0.18 nm^{-2}.) Neglecting the region of dangling corona ends, the radius of a nonswollen hairy sphere R_{dry} as calculated from the grafting density, the hair molecular weight, and the bulk density of PS ($\rho_{PS} = 1.05$ g/cm^3) would be 17.6 nm for system II and 14.1 nm for system III (see eq 10).

$$V_{dry} = {}^4/_3\pi {R_{dry}}^3 = {}^4/_3\pi R^3 + \rho_{PS} N_H (M_w/N_L) \quad (10)$$

For nonperturbed chain dimensions of the brush hairs, i.e., l [nm] $= 0.069 M_n^{0.5}$, one would obtain a brush thickness $l = 10.6$ nm and $l = 11.5$ nm for systems II and III, respectively. Therefore, the "ideal" brush size would be $R_{id} = 22.4$ nm for system II and $R_{id} = 22.2$ nm for system III.

Table 7. Comparison of the Size of a Completely Dry and an Ideal Brush with the Size at the Liquid−Solid Transition for Systems II and III, Both in a PS Matrix of $M = 3800$ g/mol

sample	R_{dry} [nm]	R_{id} [nm]	R_{eff} [nm]
system II	17.6	22.4	23.4
system III	14.1	22.2	15.7

If our free-volume approach (eq 1) is valid, in matrix $M_{PS} = 3800$ g/mol the volume swelling ratio at the liquid−solid transition can be calculated by direct comparison with the hard-sphere reference value $\phi_{0,HS} = 0.65$: one gets $0.65/0.277 = 2.35$ for system II and $0.65/0.47 = 1.38$ for system III. The effective particle radius at the liquid−solid transition R_{eff} therefore is 23.4 nm ($17.6 \times 2.35^{0.333}$) for system II and 15.7 nm ($14.1 \times 1.38^{0.333}$) for system III. If we neglect the region of dangling corona ends at the liquid−solid transition, assuming this part of the hairy particles to be fully compressed at the liquid−solid transition, these radii should correspond more or less directly to the sum of the colloidal core radius and the swollen corona region with homogeneous density profile. For comparison, the particle size at close packing R_{eff}, the size of a perfectly dry brush (R_{dry}), and the size of a brush containing nonstretched hairs (R_{id}) have been summarized in Table 7. We have calculated R_{eff} on the basis of our free volume approach, which assumes an isotropic distribution of particles showing repulsive interactions. For quantification, the hard-sphere system is used as the simplest case of such isotropic particles systems with interparticle repulsion. If any system which can be described by our approach exhibits a liquid−solid transition at a volume fraction $\phi_0 < 0.65$ (the volume fraction at random close packing of slightly polydisperse ($\Delta R/R \approx 0.1$) hard spheres),[34] this is interpreted as swelling of the particle size by the surrounding solvent or matrix and a corresponding increase in effective particle concentration. In this context, both systems II and III show this swelling as can be seen clearly by $R_{eff} > R_{dry}$. On the other hand, comparison of unperturbed brush size R_{id} and effective brush size R_{eff} shows that the hairs in the case of system II are strongly stretched, which is also to be expected for a brush with such high grafting density. For system III, $R_{eff} < R_{id}$, which means the hairs are collapsed onto the particle surface ("mushroom regime").

According to the SCF calculations of Lin and Gast,[11] at given core size and given hair length one would expect the effective particle size to increase with grafting density, whereas the softness of the repulsive interactions should decrease. This prediction corresponds well to the values of R_{eff} and κ/ϕ_0 given in Tables 7 and 6, respectively.

We can continue our calculations to deduce the "grafting density" of the dangling ends, which is given directly by the number of hairs (assuming each hair to contribute to the outer region of the particles) and the surface area of the swollen particles at the liquid−solid transition. One gets 0.062 nm^{-2} for system II and 0.048 nm^{-2} for system III. The reader should note that the grafting densities with respect to the colloidal core were 0.24 and 0.10 nm^{-2}, respectively. In comparison, the effective grafting densities of dangling ends are very similar for the two different systems II and III. Therefore, if the particle softness really is determined by the compression of the layer of dangling corona ends, the comparable κ parameters of systems II and III are not surprising anymore: both particles have comparable

Table 8. Size Swelling $(\phi_{HS}/\phi)^{0.333}$ as a Function of Effective Hard-Sphere Volume Fraction ϕ_{HS} for Grafted Microgel Systems I, II, and III in Matrix M = 3800 g/mol and for Wet-Brush Copolymer Micelles in M = 22 000 g/mol (SI, 22000)

ϕ_{HS}	0.10	0.20	0.30	0.40	0.50	0.60	0.65
$(\phi_{HS}/\phi)^{0.333}$ (I, 3800)	0.96	1.03	1.09	1.14	1.19	1.23	1.25
$(\phi_{HS}/\phi)^{0.333}$ (II, 3800)	1.18	1.21	1.23	1.26	1.29	1.31	1.32
$(\phi_{HS}/\phi)^{0.333}$ (III, 3800)	1.22	1.20	1.18	1.16	1.14	1.12	1.11
$(\phi_{HS}/\phi)^{0.333}$ (SI, 22000)	1.41	1.37	1.33	1.29	1.25	1.20	1.18

densities of dangling ends. In this discussion, the effect of surface curvature is neglected. Also, it is very difficult to make an assumption about the length of the dangling ends. One only might speculate that the inner corona region (swollen corona with constant density profile) basically consists of interentangled corona chains. Since the entanglement molecular weight of PS is about 10 000 g/mol, the dangling ends should definitely be much smaller than 10 000 g/mol, the more since in the case of the grafted microgels the total hair length is only about 25 000 g/mol.

5. Dependence of Particle Volume Swelling on Concentration. For particles interacting via a repulsive potential, it should be possible to determine the effective particle size (with respect to the size of a nonswollen spherical brush) as a function of particle concentration simply by solving the following equation:

$$\frac{\tau_0}{\tau} = \exp\left(-\frac{\kappa}{\phi^{-1} - \phi_0^{-1}}\right) = \exp\left(-\frac{1.60}{\phi_{HS}^{-1} - 0.65^{-1}}\right) \tag{11}$$

Here, by directly comparing the mobility of a given sample with the hard-sphere reference, we assume that identical normalized structural relaxation times correspond to identical effective hard-sphere volume fractions ϕ_{HS}. This also comprises the assumption that, at a given concentration, our soft-particle system and the hard-sphere reference have a comparable isotropic structure or radial particle density distribution. As a direct consequence, a particle volume fraction of ϕ (nonswollen brush) corresponds to an effective hard-sphere particle volume fraction ϕ_{HS}, and the degree of particle swelling is simply given by the ratio ϕ_{HS}/ϕ. Note, however, that this simplified approach treats also strongly swollen wet-brush systems, at a given concentration, as if they would effectively interact via a hard-sphere potential. Particle softness, that is, compressibility and/or deformability in this context, causes a decrease of the effective hard-sphere radius with increasing micelle concentration. If we solve eq 11 with the fitting parameters given in Table 6, we directly obtain the swelling in particle size in dependence of particle concentration, that is, $(\phi_{HS}/\phi)^{0.333}(\phi)$. Results are summarized for systems I, II, and III in matrix polymer M = 3800 g/mol in Table 8, where, for comparison, the concentration dependence of the size swelling of the previously studied copolymer micelles also is shown.

As expected for wet-brush particles with a soft-repulsive potential and the resulting isotropic homogeneous particle distribution, the copolymer micelles (SI, 22K) show a continuous decrease in effective particle size with increasing particle concentration and, correspondingly, increasing particle interactions.

On the other hand, the grafted microgels exhibit a very surprising behavior, which is consistent with the very small κ values given in Table 6. Especially systems I and II behave very unusual: being even more strongly swollen at the liquid−solid transition (ϕ_{HS} = 0.65) than the micellar wet-brush, the degree of size swelling decreases with decreasing concentration. On the other hand, the particles seem to increase in effective size with increasing particle interactions. This behavior is very counterintuitive and even nonphysical, since increasing interparticle interactions should rather compress the particle hair layer than cause its expansion. It seems that the densely grafted microgel systems I and II, although strongly swollen by the matrix polymer chains (as deduced from the location of the liquid−solid transition) and therefore in this respect resembling wet spherical brushes, nevertheless in contrast to the previously studied micellar system cannot be mapped onto an effective hard-sphere reference system. Therefore, we may conclude that our assumptions in applying the Doolittle equation are not fulfilled for these densely grafted particles. Most plausibly, the particles are not homogeneously distributed all over the sample at very high concentrations as expected for a simple repulsive system, but form clusters. In this case, the liquid−solid transition might be based rather on gelation due to a network of such clusters than on a glass transition corresponding to an isotropic random close packing as expected for simple repulsive polydisperse hard-sphere systems. Such gels usually are formed if the interparticle interaction pair potential is attractive. One only might speculate that the high grafting density in combination with the comparatively short hair length causes such attractive particle interactions.

Finally, let us consider system III. Although being definitely swollen (size swelling 1.22−1.11 (see Table 8), ϕ_0 = 0.47 (see Table 6), the degree of swelling in comparison to the micellar system is less dependent on particle concentration and also quite small compared to systems with higher grafting density. This reflects a comparatively hard-sphere character of system III: because of swelling by the matrix polymer, the particle size is increased by about 20%. A size compression of only about 10% is found with increasing concentration up to the liquid−solid transition. Because of the low grafting density and the large ratio of hair to chain length, system III is expected to show the soft-repulsive potential of a wet brush. The short length of the hairs with respect to the overall particle size in addition to a collapse of the grafted layer onto the particle core, leading to comparatively small particle volume swelling (mushroom regime, see also Figure 7), however, seems to lead to a rather steep hard-sphere-like repulsion.

Conclusions

We have investigated the dynamic mechanical behavior of spherical brushes embedded in a homopolymer melt, extending our previous studies of copolymer micelles to polymer grafted microgels with much shorter hair and various grafting densities. The structural relaxation time as a function of particle concentration has been analyzed by a free volume approach. To quantify the softness of the interparticle interaction potential and the effective particle size, fitting results have been compared to the well-known hard-sphere reference system. Surprisingly, the κ parameter of the Doolittle equation, characterizing the particle softness, has been found to be considerably smaller for the new microgel system with respect to the copolymer micelles.

By determining the effective particle volume at the liquid−solid transition with respect to the hard-sphere value $\phi_{0,HS} = 0.65$, we found that the particle swelling increases with both increasing hair length and increasing grafting density. A more detailed analysis of effective particle size vs particle concentration showed that fitting the structural relaxation dynamics of highly grafted spherical brushes to a free volume model led to nonphysical results for the densely grafted microgel systems, that is, an increase of the effective particle volume with increasing particle concentration. This leads to the conclusion that densely grafted spherical brushes with comparatively short hairs cannot be described as effectively repulsive particles, but should have a more complicated interaction pair potential with presumably additional attractive contributions. Finally, spherical brush particles with very low grafting density and comparatively short hairs have been found to exhibit much less swelling in particle volume than expected and a comparatively steep repulsive interaction potential, which has been explained in terms of a collapse of the brush layer onto the particle core. Our studies hopefully have provided some deeper insight into the delicate effects of hair length, grafting density, and last but not least matrix chain length on the effective particle size and interaction pair potential of spherical polymer brushes in a homopolymer chain matrix.

Acknowledgment. This work was financially supported by the Deutsche Forschungsgemeinschaft (Grant SFB 262, Project D23). Rheological measurements have been performed at the Max-Planck-Institut für Polymerforschung, Mainz, with the support of Dr. T. Pakula.

References and Notes

(1) Gohr, K.; Pakula, T.; Tsutsumi, K.; Schärtl, W. *Macromolecules* **1999**, *32*, 7156−7165.
(2) Gohr, K.; Schärtl, W. *Macromolecules* **2000**, *33*, 2129−2135.
(3) Doolittle, A. K. *J. Appl. Phys.* **1951**, *22*, 1471−1475.
(4) Graf, C.; Schärtl, W.; Maskos, M.; Schmidt, M. *J. Chem. Phys.* **2000**, *112*, 3031−3039.
(5) Woodcock, L. V.; Angell, C. A. *Phys. Rev. Lett.* **1981**, *47*, 1129−1132.
(6) Leibler, L.; Pincus, P. A. *Macromolecules* **1984**, *17*, 7, 2922−2924.
(7) Buscall, R.; Dhaene, P.; Mewis, J. *Langmuir* **1994**, *10*, 1439−1441.
(8) Frith, W. J.; dHaene, P.; Buscall, R.; Mewis, J. *J. Rheol.* **1996**, *40*, 531−548.
(9) Graham, A. L. *Appl. Sci. Res.* **1981**, *37*, 275−286.
(10) Krieger, I. M. *Adv. Colloid Interface Sci.* **1972**, *3*, 111−136.
(11) Lin, E. K.; Gast, A. P. *Macromolecules* **1996**, *29*, 390−397.
(12) Vrij, A. *Pure Appl. Chem.* **1976**, *48*, 471−483.
(13) Asakura, S.; Oosawa, F. *J. Chem. Phys.* **1954**, *22*, 1255−1256.
(14) Joanny, J. F.; Leibler, L.; de Gennes, P. G. *J. Polym. Sci., Part B: Polym. Phys.* **1979**, *17*, 1073−1084.
(15) Alexander, S. *J. Phys. (Paris)* **1977**, *38*, 977−981.
(16) de Gennes, P. G. *Macromolecules* **1980**, *13*, 1069−1075.
(17) Wijmans, C. M.; Zhulina, E. B. *Macromolecules* **1993**, *26*, 7214−7224.
(18) Wijmans, C. M.; Zhulina, E. B.; Fleer, G. J. *Macromolecules* **1994**, *27*, 3238−3248.
(19) Milner, S. T. *Science* **1991**, *251*, 905−914.
(20) Daoud, M.; Cotton, J. P. *J. Phys. (Paris)* **1982**, *43*, 531−538.
(21) Wijmans, C. M.; Leermakers, F. A. M.; Fleer, G. J. *Langmuir* **1994**, *10*, 4514−4516.
(22) Roan, J. R.; Kawakatsu, T. *J. Chem. Phys.* **2002**, *116*, 7295−7310.
(23) Grest, G. S. *J. Chem. Phys.* **1996**, *105*, 5532−5541.
(24) Gay, C. *Macromolecules* **1997**, *30*, 5939−5943.
(25) Martin, J. I.; Wang, Z.-G. *J. Phys. Chem.* **1995**, *99*, 2833−2844.
(26) Aubouy, M.; Fredrickson, G. H.; Pincus, P.; Raphael, E. *Macromolecules* **1995**, *28*, 2979−2981.
(27) Ferreira, P. G.; Ajdari, A.; Leibler, L. *Macromolecules* **1998**, *31*, 3994−4003.
(28) Hasegawa, R.; Aoki, Y.; Doi, M. *Macromolecules* **1996**, *29*, 6656−6662.
(29) Baumann, F.; Schmidt, M.; Deubzer, B.; Geck, M.; Dauth, J. *Macromolecules* **1994**, *27*, 6102−6105.
(30) Perruchot, C.; Khan, M. A.; Kamitsi, A.; Armes, S. P. *Langmuir* **2001**, *17*, 4479−4481.
(31) Ferry, J. D. *Viscoelastic Properties of Polymers;* Wiley & Sons: New York, 1980.
(32) Ninomiya, K.; Ferry, J. D. *J. Colloid Sci.* **1959**, *14*, 36.
(33) Watanabe, H.; Sato, T.; Osaki, K.; Hamersky, M. W.; Chapman, B. R.; Lodge, T. P. *Macromolecules* **1998**, *31*, 3740−3742.
(34) Schaertl, W.; Sillescu, H. *J. Stat. Phys.* **1994**, *77*, 1007−1025.
(35) Förster, S.; Wenz, E.; Lindner, P. *Phys. Rev. Lett.* **1996**, *77*, 95.

MA021179W